Supplementary Information

The multiple MMCT properties of a diruthenium-based cyanido-bridged complex Ru_2^{VI}-NC-Ru^{II}-CN-Ru_2^{VI}

Shao-Dong Su, [1] Yue-Hong Wen, [1] Xin-Tao Wu, [1] and Tian-Lu Sheng*[1]

[1]State Key Laboratory of Structural Chemistry, Fujian Institute of Research on the Structure of Matter, Chinese Academy of Sciences, Fuzhou 350002, People's Republic of China

Table of Contents

1. Crystallographic data

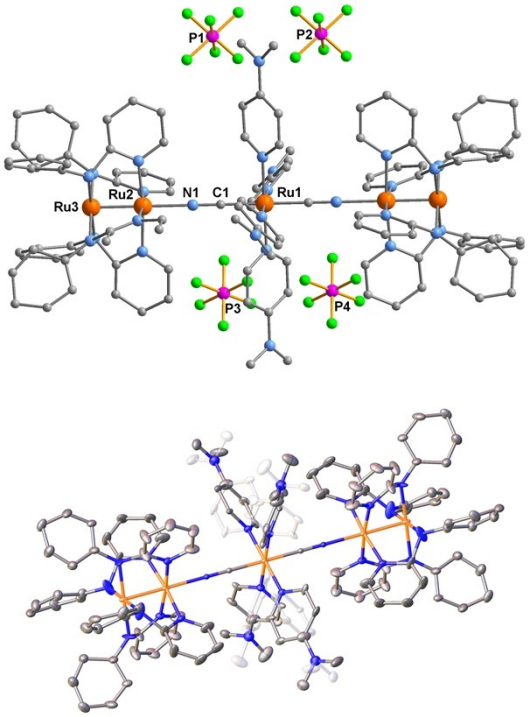

Figure S1. The structural diagram of complex $1^{4+}[PF_6]_4$ (top) and 1^{4+} with the disorder atoms displayed in shadow (bottom). [Orange(Ru), blue(N), grey(C), purple(P), green(F), H atoms have been omitted for clarity.]

Table S1. Crystallographic data and a summary of the structural refinements for complex $1^{2+}[PF_6]_2$

Complex	$1^{2+}[PF_6]_2 \cdot 2.5\ CH_2Cl_2$
Empirical formula	C120.5 H117 F12 N26 P2 Ru5 Cl5
Color	green
Crystal system	Triclinic
Space group	P -1
a (A)	11.672(5)
b (A)	11.727(5)
c (A)	24.284(9)
alpha (deg.)	81.355(14)
beta (deg.)	87.766(14)
gamma (deg.)	89.663(11)
Volume(A^3)	3284(2)
Z	1
Formula weight	2901.93
Density(cal.)(Mg/m^3)	1.468
Absorption coefficient(mm^-1)	0.761
Temperature(K)	100(2)
Theta range (deg.)	2.388 to 24.998

Reflections measured	**41879**
Independent reflections	**11457**
Observed Reflection	**8648**
Final R indices (obs.)	**R1 = 0.0829, wR2 = 0.1974**
R indices (all)	**R1 = 0.1070, wR2 = 0.2160**
Goodness-of-fit	**1.105**

$R_1 = \Sigma(||F_0| - |F_c||)/\Sigma|F_0|$;
$wR_2 = [\Sigma w(|F_0^2| - |F_c^2|)^2/\Sigma w|F_0^2|^2]^{1/2}$

Table S2. Crystallographic data and a summary of the structural refinements for complex $1^{4+}[PF_6]_4$

Complex	**$1^{4+}[PF_6]_4$**
Empirical formula	**C118 H112 F24 N26 P4 Ru5**
Color	**purple**
Crystal system	**Tetragonal**
Space group	**I 4/m**
a (A)	**14.352(2)**
b (A)	**14.352(2)**
c (A)	**33.260(7)**
alpha (deg.)	**90**
beta (deg.)	**90**
gamma (deg.)	**90**
Volume(A^3)	**6851(2)**
Z	**2**
Formula weight	**2979.56**
Density(cal.)(Mg/m^3)	**1.444**
Absorption coefficient(mm^-1)	**0.672**
Temperature(K)	**100(2)**
Theta range (deg.)	**1.499 to 25.364**
Reflections measured	**16352**
Independent reflections	**3064**
Observed Reflection	**2509**
Final R indices (obs.)	**R1 = 0.1875, wR2 = 0.4048**
R indices (all)	**R1 = 0.2012, wR2 = 0.4112**
Goodness-of-fit	**1.049**

$R_1 = \Sigma(||F_0| - |F_c||)/\Sigma|F_0|$;
$wR_2 = [\Sigma w(|F_0^2| - |F_c^2|)^2/\Sigma w|F_0^2|^2]^{1/2}$

Table S3. Selected bond lengths (Å) and angles (deg.) of $1^{2+}[PF_6]_2$ and $1^{4+}[PF_6]_4$

	$1^{2+}[PF_6]_2$	$1^{4+}[PF_6]_4$
Ru(2)-Ru(3)	2.2804(12)	2.253(5)
Ru(1)-C(1)	2.076(6)	1.979(18)
Ru(2)-N(1)	2.148(6)	2.14(2)
Ru-N_{ap}-average	2.081, 2.035	2.092，2.016
Ru-N_{DMAP}	2.103	2.10(2)
C(1)-Ru(1)-N(2)	89.8(2)	92.1(7)
C(1)-Ru(1)-N(4)	90.4(3)	-
N(2)-Ru(1)-N(4)	90.1(2)	-
N(1)-C(1)-Ru(1)	179.0(6)	180.0
C(1)-N(1)-Ru(2)	179.5(6)	180.0
N(1)-Ru(2)-Ru(3)	179.91(17)	180.0

2. Magnetic measurement

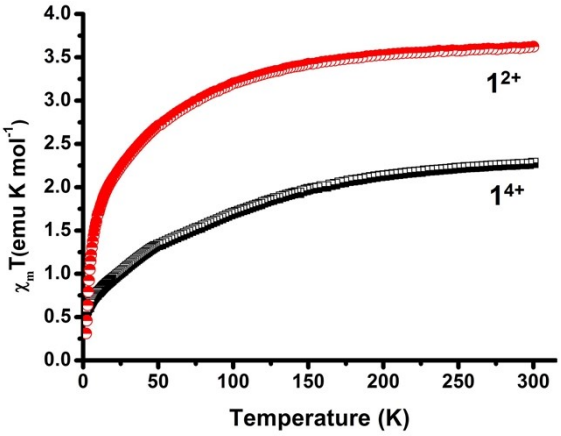

Figure S2. The variable temperature magnetic susceptibility measurement of complex 1^{2+}(red ○) and 1^{4+}(black □) in the range of 2-300K.

3. IR spectra

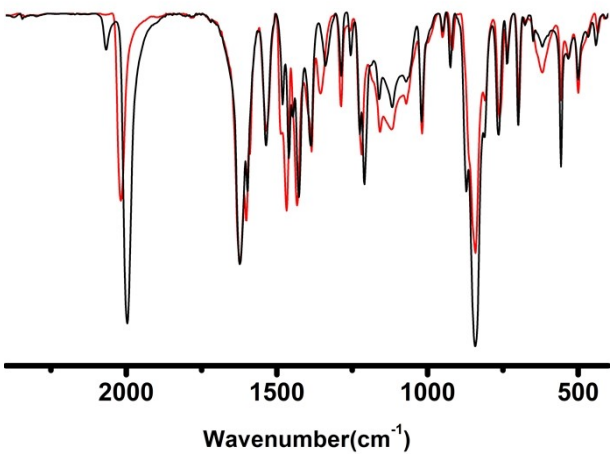

Figure S3. IR spectra of complexes $1^{2+}[PF_6]_2$ (red line) and $1^{4+}[PF_6]_4$ (black line).

4. Theoretical calculation

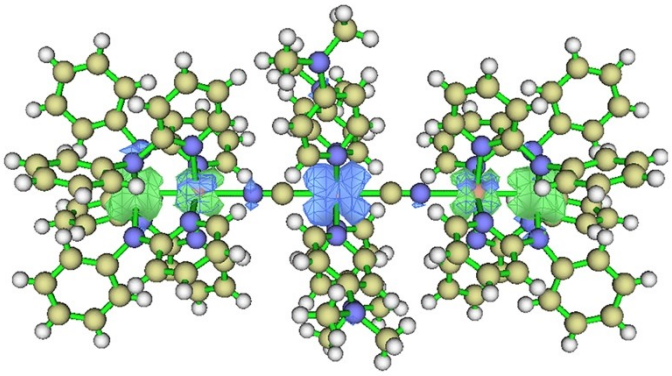

Figure S4. Redistribution of electron densities for complex 1^{2+} in the calculated MMCT transition band at 16673 cm^{-1} (f=0.0282). The green and blue areas represent gain and loss of density.

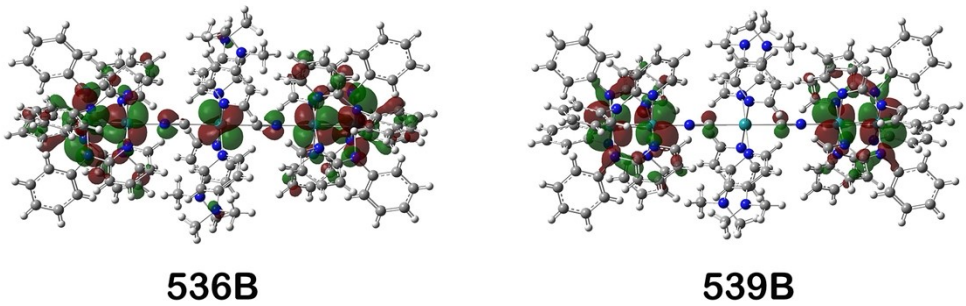

Figure S5. Molecular orbital diagrams of orbital transition HOMO-1 (536β) → LUMO+1 (539β) (0.51812) for MMCT of 1^{2+} at 16673 cm^{-1}.

Table S4. Gaussian peak fitting data of complex 1^{4+}.

	ν_{max} (ε_{max}, FWHM) [cm^{-1}($M^{-1}cm^{-1}$, cm^{-1})]		
	MMCT-1	**MMCT-2**	**MMCT-3**
1^{4+}	12715 (8848,2695)	7730 (8764,2005)	5996 (4719,2005)

Table S5. Calculated MMCT absorption bands, energy, main orbital transition, oscillator strengths of complex 1^{4+}

	absorption band (cm^{-1})	Energy (eV)	orbital transition	oscillator strengths (f)
MMCT-1	13185	1.6348	536β→542β (0.79779)	0.0207
MMCT-2	8111	1.0056	531β→542β (0.22701)	0.0108
MMCT-3	6386	0.7918	537β→538β (0.90730)	0.0136